Functional evidence of distinct ATP activation sites at the human $P2X_7$ receptor

Manuela Klapperstück, Cora Büttner*, Günther Schmalzing*† and Fritz Markwardt

*Julius-Bernstein-Institut für Physiologie, Martin-Luther-Universität Halle-Wittenberg, Magdeburger Straße 6, D-06097 Halle/Saale, *Pharmakologisches Institut für Naturwissenschaftler, Biozentrum N260, Johann-Wolfgang-Goethe-Universität Frankfurt/Main, Marie-Curie-Straße 9, D-60439 Frankfurt/Main and † Institut für Experimentelle und Klinische Pharmakologie, Albert-Ludwigs-Universität Freiburg, Hermann-Herder-Straße 5, D-79104 Freiburg, Germany*

(Received 21 November 2000; accepted after revision 4 March 2001)

1. The effect of the agonist ATP on whole cell currents of *Xenopus* oocytes expressing either the wild-type human $P2X_7$ receptor ($hP2X_7$), an N-terminally hexahistidyl-tagged $hP2X_7$ receptor (His-$hP2X_7$), or a truncated His-$hP2X_7$ receptor (His-$hP2X_7\Delta C$) lacking the C-terminal 156 amino acids was investigated using the two-microelectrode voltage clamp technique.

2. The activation time course of the wild-type $hP2X_7$ receptor can be described as the sum of an exponentially growing and an additional almost linearly activating current component.

3. The amplitude of the exponentially activating current component of the wild-type $hP2X_7$ receptor displayed a biphasic dependence on the agonist concentration, which could be best approximated by a model of two equal high-sensitivity and two equal low-sensitivity non-cooperative activation sites with apparent dissociation constants of about 4 and 200 μM free ATP^{4-}, respectively.

4. The linearly activating current was monophasically dependent on the agonist concentration with an apparent dissociation constant of about 200 μM.

5. The contribution of the low-sensitivity sites to current kinetics was reduced or almost abolished in oocytes expressing His-$hP2X_7$ or His-$hP2X_7\Delta C$.

6. Our data indicate that the $hP2X_7$ receptor possesses at least two types of activation sites, which differ in ATP^{4-} sensitivity by a factor of 50. The degree of occupation of these two sites influences both activation and deactivation kinetics. Both N- and C-terminal domains appear to be important determinants of the current elicited by activation of the sites with low ATP sensitivity, but not for that mediated by the highly ATP-sensitive sites.

Many effects of extracellular ATP on cells of the immune system have been attributed to the presence of a so-called P2Z receptor. Recent work has shown that one of the members of the P2X family of ATP-gated receptors (Buell *et al.* 1996; Soto *et al.* 1997; Ralevic & Burnstock, 1998; MacKenzie *et al.* 1999), designated $P2X_7$, shares many phenotypical properties with the P2Z receptor upon heterologous expression, suggesting that the two are identical. The $P2X_7$ receptor is therefore also referred to as P2Z/$P2X_7$ receptor (Di Virgilio, 1995; Di Virgilio *et al.* 1998). A peculiarity of the $P2X_7$ subunit is its very long intracellular C-terminal tail, which is 196 or 132 amino acids longer than that of the $P2X_1$ or $P2X_2$ subunit isoform, respectively.

Several studies attempting to characterise the recombinant $P2X_7$ receptor have provided information about its complex function, which is not yet fully understood. During short applications of ATP lasting a few seconds, the $P2X_7$ receptor behaves like a typical P2X family member, exhibiting permeability to small cations only. However, upon prolonged or repeated applications of ATP, large non-selective pores are formed in the plasma membrane of some cells expressing $P2X_7$ (Surprenant *et al.* 1996; Rassendren *et al.* 1997; Virginio *et al.* 1999), which have been attributed to the receptor itself. On the other hand, it has also been suggested that the pores represent distinct entities, which become activated subsequent to the stimulation of $P2X_7$ receptors (Coutinho-Silva & Persechini, 1997; Schilling *et al.* 1999).

In native cells, ATP elicits different effects over a wide concentration range. For instance, ATP increases the cell

membrane permeability in T lymphocytes, but does not cause lysis at concentrations below 100 μM (El-Moatassim *et al.* 1989), whereas in the millimolar range ATP induces cytolysis and the subsequent death of T lymphocytes (Di Virgilio *et al.* 1989; Filippini *et al.* 1990; Zanovello *et al.* 1990). Furthermore, immunomodulatory effects, such as the inhibition of human natural killer cell reactivity (Schmidt *et al.* 1984) and the inhibition of macrophage-mediated cytotoxicity (Cameron, 1984), have been observed to occur at $<$ 100 μM ATP, whereas at least 500 μM ATP was necessary for ATP-induced killing of mycobacteria by human macrophages (Lammas *et al.* 1997). In addition to the induction of cytolytic pores in some cell types of the immune system, P2Z receptor-dependent activation of phospholipase D (Dubyak & El-Moatassim, 1993), NFkB (Ferrari *et al.* 1997) and interleukin-1β-converting enzyme (Di Virgilio *et al.* 1998) have been described, as has the P2Z receptor-dependent loss of L-selectin from human lymphocytes (Jamieson *et al.* 1996).

The molecular basis for the distinct behaviour of immune cells over a broad ATP concentration range is still unclear and may simply reflect the modification of the internal milieu by the concentration-dependent permeabilising effect of $P2X_7$ receptor activation. The various cellular responses may thus be triggered by quantitatively different changes in the intracellular Ca^{2+}, Na^+ or K^+ concentrations due to $P2X_7$ receptor stimulation. Thus the degree of ATP breakdown by ectoATPases, the amount of receptor expression in the investigated cells and the concentration of divalent cations reducing the concentration of the ligand, free ATP^{4-} (Di Virgilio *et al.* 1998), has to be taken into account. Furthermore, the possible involvement of other receptors with different sensitivity to ATP has to be considered.

Here we provide electrophysiological evidence of distinct ATP activation sites at the human $P2X_7$ receptor. The two sites differ in their ATP sensitivity by a factor of about 50 and influence differently both the activation and deactivation kinetics and the permeation characteristics of the $hP2X_7$ receptor. The existence of two ATP activation sites provides one possible explanation for the variable pattern of signalling of $hP2X_7$-expressing cells at different concentrations of ATP.

METHODS

Chemicals

Chemicals were obtained from Sigma (Deisenhofen, Germany) unless stated otherwise.

cDNA constructs

The isolation of a human $P2X_7$ cDNA by RT-PCR from human B lymphocytes has been described previously (Klapperstück *et al.* 2000). The deduced amino acid sequence deviates in two positions (G441 and A496) from the sequence published under accession no. Y09561. His-$P2X_7$ was created by inserting codons for six tandem histidine residues (His) without changing any other amino acid at an engineered *Nco*I cleavage site just behind the initiating ATG. Site-directed mutagenesis was achieved by using the QuikChange system (Stratagene). His-$hP2X_7$-ΔC encoding a truncated mutant of His-$hP2X_7$ lacking the uttermost 156 C-terminal amino acids was generated by inserting a stop codon between an intrinsic *BspM*I cleavage site and an *Apa*I site in the 3′ non-coding region. All mutations, inserted oligonucleotides and junction sequences were confirmed by nucleotide sequencing (Sanger *et al.* 1977).

cRNA synthesis

Capped cRNAs were synthesised from linearised templates with SP6 RNA polymerase (Pharmacia), purified by sepharose chromatography and phenol–chloroform extraction (Yisraeli & Melton, 1989), and dissolved in 5 mM Tris-HCl, pH 7.2, at 0.5 μg μl^{-1}, using the optical density (OD) reading at 260 nm for quantitative analysis (OD 1.0 = 40 μg μl^{-1}).

Oocyte treatment

The experiments followed national guidelines on animal experimentation. *Xenopus laevis* females were imported from the African *Xenopus* Facility (Knysna, Republic of South Africa). The animals were anaesthetised in an aqueous solution supplemented with 5 mM Hepes and 5 mM tricaine (MS222). Parts of the ovary were removed through a small incision and kept overnight in normal Barth's solution (mM): NaCl 100, KCl 1, $MgCl_2$ 1, $CaCl_2$ 1; pH 7.4 with NaOH, supplemented with 1.5 mg ml^{-1} collagenase for defolliculation. After several washes in nominally Ca^{2+}-free Barth's solution, the oocytes were placed in Petri dishes containing normal Barth's solution. Stage V or VI oocytes were injected with 20–50 nl of cRNA and then kept in normal Barth's solution supplemented with antibiotics (10 000 U ml^{-1} penicillin, 10 mg ml^{-1} streptomycin) at 19 °C until used 2–4 days later. Frogs were killed after the final oocyte collection.

Electrophysiology

All experiments were carried out at room temperature (~22 °C). Fast and reproducible solution exchange was achieved using a small tube-like chamber (0.1 ml) combined with fast superfusion (~75 μl s^{-1}). Switching between different bathing solutions was performed by a set of computer-controlled magnetic valves using a modified U-tube technique (Bretschneider & Markwardt, 1999). The measurement of membrane currents was performed using the two-microelectrode voltage clamp method. Microelectrodes were pulled from borosilicate glass and filled with 3 M KCl. Only electrodes with resistances of between 0.5 and 1 MΩ were used. Currents were recorded and filtered at 100 Hz using an oocyte clamp amplifier (OC-725C, Hamden, USA) and sampled at 85 Hz. Data were stored and analysed on a personal computer using software programmed at our department (Superpatch 2000, SP-Analyzer by T. Böhm).

The impalement and measurement of the membrane potential of the oocytes was carried out in normal oocyte Ringer solution containing (mM): NaCl 100, KCl 2.5, $MgCl_2$ 1, $CaCl_2$ 1; pH 7.4 with NaOH. Subsequent measurements of $hP2X_7$ receptor-dependent currents were in most cases carried out in Ca^{2+}-free, Mg^{2+}-free bathing solutions (supplemented with 0.1 mM EGTA) at a holding potential of −40 mV, unless indicated otherwise. Ca^{2+} was omitted to avoid activation of endogenous currents by Ca^{2+} influx through $hP2X_7$ receptor channels. Mg^{2+} was omitted to prevent Mg^{2+} complexation of ATP^{4-}, since otherwise the high ATP concentrations required for maximal activation of the $hP2X_7$ receptor would have been insoluble (Di Virgilio, 1995; Markwardt *et al.* 1997). This means that in these solutions, the concentrations of the total ATP and of the free ATP^{4-} are approximately the same. The removal of divalent cations from the extracellular solution evoked a large conductance, which could be blocked by the non-selective cation channel blocker 0.1 mM flufenamic acid (Weber *et al.* 1995; Zhang *et al.* 1998). In some experiments, 1 mM Ba^{2+} was used as a divalent cation instead of Ca^{2+},

since Ba^{2+} has been reported to block Ca^{2+}-induced Cl^- currents (Barish, 1983). For bathing solutions containing divalent cations, the total ATP concentration required to achieve a desired ATP^{4-} concentration was calculated by a computer program kindly provided by R. Schubert (Schubert, 1990).

In control oocytes injected with H_2O, 1 mM extracellular ATP induced no, or very small (< 1 nA) inward, currents. In some cases larger currents (< 4 nA) were recorded, but only after the first application of ATP.

Non-linear approximations and presentation of data were performed using the program SigmaPlot (Jandel, Corte Madeira, USA). Averaged data are given as means ± S.D. unless stated otherwise. Statistical data were analysed by one-way ANOVA. Statistical significance of differences between means was tested using the multiple *t* test (Bonferroni) by the program SigmaStat (Jandel). Significance was taken at $P < 0.05$.

RESULTS

Dependence of the activation and deactivation time courses of the hP2X$_7$ receptor on agonist concentration

Figure 1*A–C* shows the time courses of ion currents in oocytes expressing the wild-type hP2X$_7$ receptor before, during (activation) and after (deactivation) extracellular application of ATP. With increasing agonist concentrations, an apparently linearly activating component became increasingly more prominent in addition to the exponentially activating current. Furthermore, at high ATP concentrations the deactivation is apparently accelerated. For quantitative analysis, the activating part of the hP2X$_7$ receptor current ($I_{act}(t)$) was fitted according to:

$$I_{act}(t) = I_{act,\infty}(1 - \exp(-(t/\tau_{act}))) + s\,t + I_0, \quad (1)$$

where $I_{act,\infty}$ is the steady-state amplitude of the exponentially activating current after infinite time of agonist application, τ_{act} the activation time constant, s the slope of the linearly rising current, and I_0 the steady-state current without ATP application. The ratio $s/I_{act,\infty}$ increases with rising concentrations of ATP, indicating a larger contribution of the linearly activating current component (see Fig. 1 legend).

The best approximation of the deactivating current ($I_{deact}(t)$) during washout of ATP was achieved by use of:

$$I_{deact}(t) = I_{deact,1}\exp(-(t/\tau_{deact,1})) + I_{deact,2}\exp(-(t/\tau_{deact,2})) + I_0, \quad (2)$$

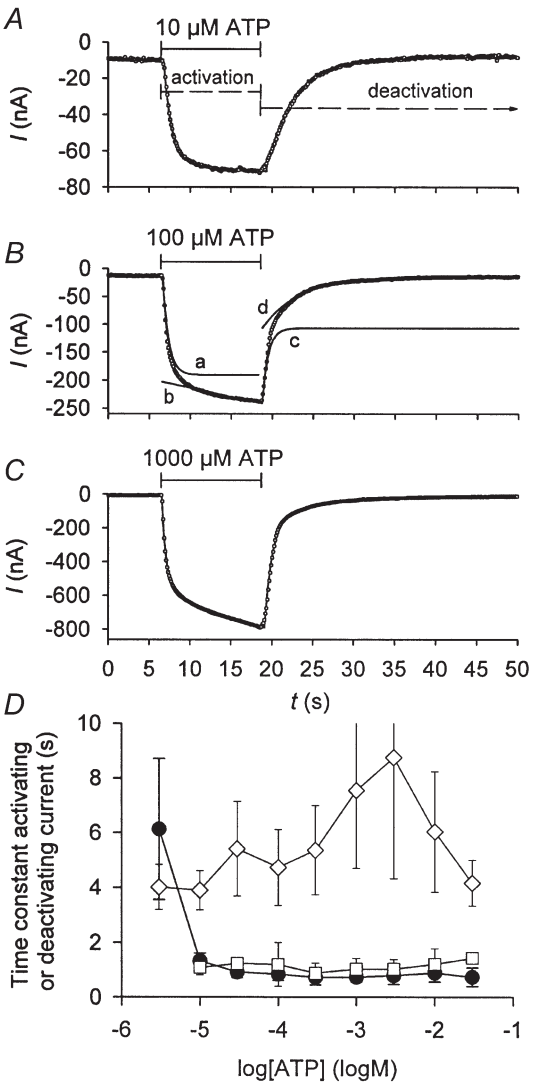

Figure 1. Dependence of hP2X$_7$ kinetics on the agonist concentration

A–C, examples of ATP-dependent currents elicited by different concentrations of ATP as indicated. All recordings were obtained from the same oocyte. Divalent cation-free oocyte Ringer solution (see Methods) was used as bathing solution. ○——○, measured currents and the approximations of their time course. Activation and deactivation were approximated according to eqns (1) and (2), respectively. *A*, the activation and deactivation time courses are marked. *B*, the exponentially (a) and the linearly (b) activating, as well as the fast (c) and slowly (d) deactivating, current components are depicted as additional lines. The relation of the slope of the linearly activating current to the steady-state amplitude of the exponentially activating current, $s/I_{act,\infty}$, was calculated as 0.006, 0.017 and 0.031 s^{-1} and the relation of the initial amplitudes of the fast and slow deactivating current, $I_{deact,2}/I_{deact,1}$, was determined as 0, 1.5 and 5.1 for *A*, *B* and *C*, respectively. For statistics, see Fig. 2, and Table 1. *D*, dependence of the activation time constant, τ_{act} (●), and of the deactivation time constants $\tau_{deact,1}$ (◇) and $\tau_{deact,2}$ (□) on the concentration of ATP. Data points represent means of between 5 and 25 oocytes.

where I_0 is the steady-state current without ATP as in eqn (1), $I_{deact,1}$ and $I_{deact,2}$ are the initial amplitudes and $\tau_{deact,1}$ and $\tau_{deact,2}$ are the time constants of the slowly and fast deactivating component, respectively. As shown in Fig. 1*D*, the time constant for activation is, at least for low agonist concentrations, critically dependent on the concentration of ATP. However, the deactivation time constants are independent of the ATP concentration (correlation coefficients were not significantly different from 0). A more detailed kinetic analysis is hampered by the slow solution exchange system (Klapperstück *et al.* 2000) which is rate limiting for time constants < 1 s. The activation and deactivation time constants for ATP of the mutant receptors His-hP2X$_7$ and His-hP2X$_7$ΔC (see below) are not significantly different from the wild-type hP2X$_7$ receptor (data not shown).

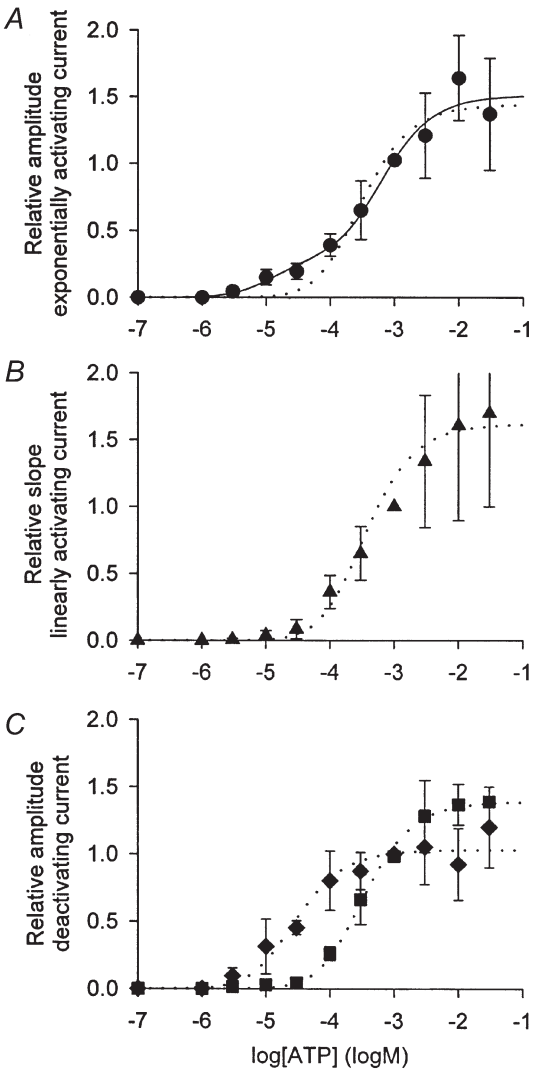

Figure 2. ATP concentration dependence of different hP2X$_7$ current components

Concentration–response curves of the steady-state activating current, $I_{act,\infty,rel}$ (*A*), of the slope of the linearly activating current, s_{rel} (*B*), and of the slow and fast deactivating current components, $I_{deact,1,rel}$ and $I_{deact,2,rel}$ (*C*), normalised to the corresponding values at 1 mM ATP. Data points represent means from between 5 and 25 oocytes. Mean data were approximated by eqn (3) (dotted line) or eqn (4) (continuous line). The calculated dissociation constants are given in Table 1 (see $I_{act,\infty}$, s, $I_{deact,1}$, and $I_{deact,2}$ for hP2X$_7$). Divalent cation-free oocyte Ringer solution was used as the bathing solution.

Concentration–response curves reveal at least two activation sites with greatly different sensitivity to ATP

To account for differences in the expression level of the P2X$_7$ receptor between different oocytes, the activating or deactivating current components designated A in eqns (3) and (4) (where A could represent $I_{act,\infty}$, s, $I_{deact,1}$ or $I_{deact,2}$) were normalised to the respective components, A_{cont}, determined in the same oocyte at 1 mM ATP^{4-} (Figs 2, 3*C–D* and 7*A–B*) or 0.1 mM ATP^{4-} (Figs 3*B* and7*C*). Models with either one Hill function (eqn (3)) or two Hill functions (eqn (4)) were used to describe the concentration dependence of the relative current components, A_{rel}:

$$A_{rel}(C) = \frac{A(C)}{A_{cont}} = \frac{A_{rel,\infty}}{(1 + (10^{-\log K_D}/C)^2}, \quad (3)$$

$$A_{rel}(C) = \frac{A(C)}{A_{cont}} = \frac{A_{rel,\infty,1}}{(1 + (10^{-\log K_{D,1}}/C)^2} = \frac{A_{rel,\infty,2}}{(1 + (10^{-\log K_{D,2}}/C)^2}, \quad (4)$$

where $A_{rel,\infty}$, $A_{rel,\infty,1}$ and $A_{rel,\infty,2}$ are the maximal relative current components contributing to $A_{rel}(C)$ after saturation of the activation sites with the apparent dissociation constants K_D, $K_{D,1}$ and $K_{D,2}$, respectively, at infinite agonist concentrations. For all the data, a Hill coefficient of 2 resulted in higher correlation coefficients than models with Hill coefficients of 1 or more than 2.

Equation (3) with equal low-sensitivity non-cooperative activation sites could be used to describe the ATP concentration dependence of the linearly activating current component s, (Fig. 2*B*) and of the deactivating current components $I_{deact,1}$ and $I_{deact,2}$ (Fig. 2*C*).

For the steady-state values of the exponentially activating current component $I_{act,\infty}$, the concentration–response curve of the calculated relative amplitudes $I_{act,\infty,rel}(C)$ was approximated by a model of two different types (two high-sensitivity and two low-sensitivity) of non-cooperative activation sites (eqn (4); cf. Fig. 2*A*). This model fitted the data significantly better (Horn, 1987) than the simpler model using only one Hill function (eqn (3)).

Based on the calculated K_D values, the kinetic parameters can be separated into two groups: (i) the concentration dependency of both the steady-state amplitude of the exponentially activating current $I_{act,\infty}$ at low agonist concentrations (Fig. 2*A*) and the slowly deactivating current component $I_{deact,1}$ (Fig. 2*C*) are characterised by K_D values of about 4 μM ATP; (ii) the ATP concentration

Table 1. Dependence of hP2X$_7$ kinetics on the ATP^{4-} concentration and on mutations at the N- and C-terminal domains

		hP2X$_7$		His-hP2X$_7$		His-hP2X$_7$ΔC
Component	Divalent cations	p$K_{D,1}$	p$K_{D,2}$	p$K_{D,1}$	p$K_{D,2}$	p$K_{D,1}$
$I_{act,\infty}$	0 Ca^{2+}, 0 Mg^{2+}	5.2 ± 0.2	3.5 ± 0.2	5.7 ± 0.2	3.5 ± 0.3	5.4 ± 0.1
s		—	3.8 ± 0.2	—	3.8 ± 0.1	—
$I_{deact,1}$		—	3.8 ± 0.1	—	—	—
$I_{deact,2}$		4.9 ± 0.3	—	—	—	—
$I_{act,\infty}$	0 Ca^{2+}, 3 mM Mg_{total}	5.3 ± 0.1	3.6 ± 0.2	5.2 ± 0.1	—	5.5 ± 0.1
s		—	3.5 ± 0.3	—	—	—
$I_{act,\infty}$	0 Ca^{2+}, 0 Mg^{2+}, 1 mM free Ba^{2+}	5.7 ± 0.2	—	—	—	—

Statistics of apparent dissociation constants of ATP^{4-} for the different components of ATP-activated currents. Mean pK_D values (± S.E.M.) were approximated by eqns (3) or (4) according to Figs 2, 3 and 6. The different means of p$K_{D,1}$, like those of p$K_{D,2}$ are not statistically different, but means of p$K_{D,1}$ are significantly different from means of p$K_{D,2}$. Mg_{total}, total (bound and free) magnesium.

dependence of the second group is described by high K_D values of about 220 μM and includes the $I_{act,\infty}$ at high agonist concentrations (Fig. 2*A*), the slope s of the linearly activating current component (Fig. 2*B*) and the fast deactivating current component $I_{deact,2}$ (Fig. 2*C*).

This analysis also revealed that a relative enlargement of the fast deactivating current component with increasing ATP concentrations (Fig. 2*C*) is responsible for the apparent acceleration of the deactivation (see Fig. 1).

Biphasic activation characteristics are preserved in the presence of permeating divalent cations

Next we examined whether the biphasic kinetics and concentration–response relationships resulted from the use of extracellular solutions lacking divalent cations but containing flufenamic acid. To avoid the activation of $[Ca^{2+}]_i$-dependent ionic currents by Ca^{2+} influx through the hP2X$_7$ receptors, we used Ba^{2+} as the extracellular divalent cation. As already shown (Klapperstück *et al.* 2000), the time course of current activation of P2X$_7$ receptors by ATP^{4-} is similar in the absence and presence of divalent cations if ATP is applied for a few seconds only. Figure 3*A* demonstrates that the biphasic time course of current activation is virtually unchanged in the presence of Ba^{2+} in the bathing solution (cf. Fig. 1*B*). However, analysis of the deactivation using eqn (2) revealed a deceleration compared to divalent-free conditions. This could reflect changes in the unbinding characteristics of ATP^{4-}. But this assumption is inconsistent with the finding that the K_D for ATP^{4-} is not obviously changed by Ba^{2+} (see below) despite increased deactivation and decreased activation time constants (cf. Figs 1*B* and 2*A* with Figs 3*A* and *B*; see also Klapperstück *et al.* 2000). Alternatively, the deactivation could be slowed by an altered time course of the washout of the agonist. Ba^{2+}- and ATP-containing solutions always contained 1 mM free Ba^{2+}, variable amounts of ATP^{4-} and millimolar concentrations of BaATP^{2-}. The washout of this buffering mixture would be slower than the washout of ATP^{4-} alone in divalent-free extracellular solutions. Similar changes in the deactivation time course (data not shown) without significant changes in the ATP^{4-} sensitivity were found in Mg^{2+}-containing extracellular solutions (see below).

As in divalent-free extracellular solutions, the concentration–response curve for $I_{act,\infty}$ in the presence of 1 mM Ba^{2+} revealed at least one high-sensitivity activation site for ATP^{4-} (Fig. 3*B*). The pK_D value of this site was not significantly different from the value obtained in divalent-free solution (Table 1). A second low-sensitivity type of activation site seems to exist for $I_{act,\infty}$ and also for s, with a pK_D value of < 4. However, calculation of the exact pK_D value was not possible, because ATP^{4-} concentrations high enough to saturate the activation site could not be reached in the presence of 1 mM Ba^{2+} (see Methods).

Extracellular Mg^{2+} decreases the potency for total ATP at both the high- and low-sensitivity activation site

The finding that divalent cations shift the total ATP concentration–response relationship of P2Z/P2X$_7$ receptors to the right is generally explained by the assumption that free ATP^{4-}, rather than MgATP^{2-}, is the agonist (Di Virgilio *et al.* 1998). To test whether both types of ATP activation sites of the hP2X$_7$ receptor share this characteristic, we measured concentration–response curves for ATP in the presence of 3 mM total Mg^{2+}. As shown in Fig. 3*C* and *D*, Mg^{2+} reduces the potency of ATP at the hP2X$_7$ receptor. This was found for the biphasic $I_{act,\infty}$–[ATP] relationship (Fig. 3*C*), as well as for the monophasic s–[ATP] (Fig. 3*D*) relationship. If, however, the calculated ATP^{4-} concentrations rather than the total ATP concentrations are used, the concentration–response curves obtained in the absence and presence of external

Mg^{2+} become virtually identical. Likewise, the calculated K_D values for ATP^{4-} are not statistically different from those obtained in Mg^{2+}-free bathing solutions (Table 1).

The fast deactivating current component is related to the linearly activating current component

We conclude that the linearly activating and the fast deactivating current components are related to each other because they both display a similar dependence on ATP concentration (Figs 1 and 2). In Fig. 4 further evidence for this assumption is provided. Prolonged ATP application increased the linearly activating current component as well as the fast deactivating current component. In contrast, the slowly deactivating current component was independent of the duration of ATP application. This suggests that the activation of the $hP2X_7$ receptor at the highly ATP-sensitive site is responsible for one part of the exponentially activating current component and the slowly deactivating current component. This part of $hP2X_7$ activation seems to be complete after 3 s of ATP application.

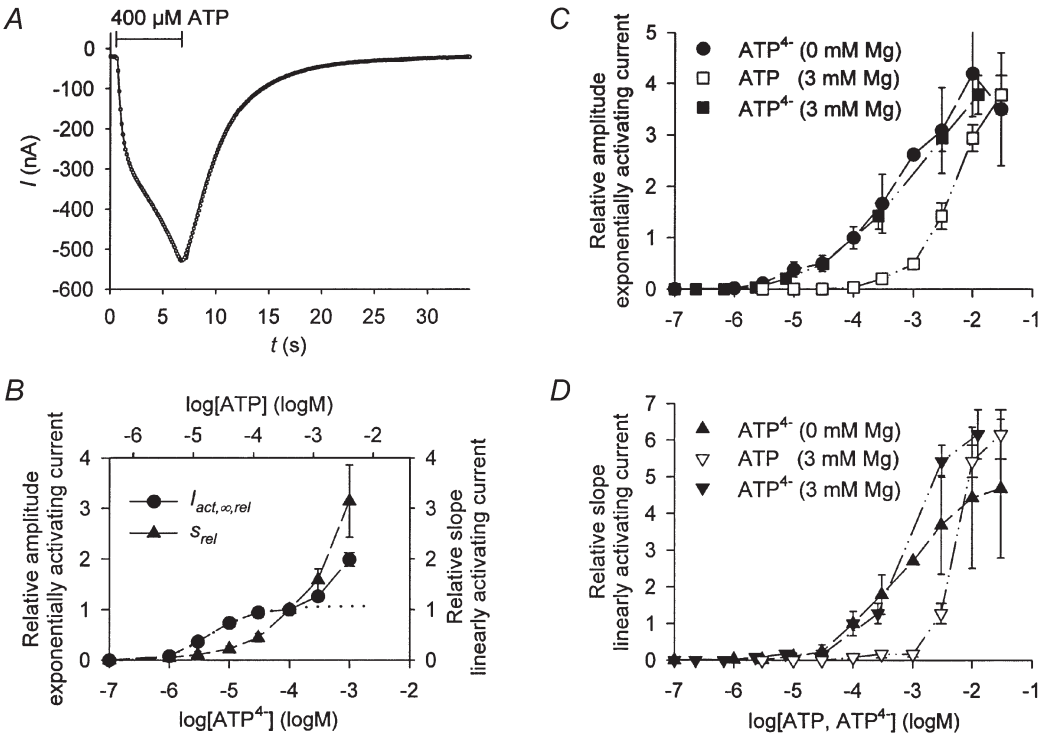

Figure 3. Kinetics of $hP2X_7$ in the presence of extracellular divalent cations

A, typical example of an ATP-dependent current elicited in 1 mM free Ba^{2+}-containing extracellular solution. Total amounts of ATP and Ba^{2+} were calculated as described in Methods to adjust the free concentrations of ATP^{4-} (as indicated) and 1 mM Ba^{2+}; 400 μM total ATP corresponds to 100 μM free ATP^{4-}. ○, measured currents (superimposed continuous line), approximated time course. Activation and deactivation were approximated according to eqns (1) and (2), respectively. The fitted parameters are: $I_{act,\infty}$, −217 nA; τ_{act}, 0.35 s; s, −47 nA s^{-1}; $I_{deact,1}$, −478 nA; $\tau_{deact,1}$, 3.5 s; $I_{deact,2}$, −37 nA; $\tau_{deact,2}$, 22 s. *B*, dependence of the steady-state activating current, $I_{act,\infty,rel}$ (●), and the slope of the linearly activating current, s_{rel} (▲), on the concentration of ATP^{4-} and total ATP in 1 mM free Ba^{2+}-containing extracellular solution (see Methods). Data are normalised to the values measured in Ba^{2+}-containing solution supplemented with 400 μM ATP. The calculated dissociation constant for $I_{act,\infty,rel}$ in the concentration range from 0.1 to 100 μM ATP^{4-} (dotted line represents fit) is given in Table 1 ($I_{act,\infty}$, 0 Ca^{2+}, 0Mg^{2+}, 1 mM free Ba^{2+}). *C* and *D*, influence of Mg^{2+} on the dependence of the $hP2X_7$-related currents on the extracellular ATP concentration. *C*, dependence of the steady-state activating current, $I_{act,\infty,rel}$ (□); *D*, the slope of the linearly activating current, s_{rel} (▽), on the total ATP concentration in extracellular solution containing 3 mM total Mg. Data were normalised to the values obtained at 1 mM ATP in divalent cation-free oocyte Ringer solution. The concentration–response curves were recalculated and redrawn using the ATP^{4-} concentration as agonist (■, $I_{act,\infty,rel}$; ▼, s_{rel}). For comparison, the concentration–response curve for ATP^{4-} obtained in Mg^{2+}-free solution (same as in Fig. 2*A* and *B*) were also shown (●, $I_{act,\infty,rel}$; ▲, s_{rel}). Data points represent means of between 5 and 25 oocytes. The dependencies of $I_{act,\infty,rel}$ and s_{rel} on ATP^{4-} measured in Mg^{2+}-containing solution were fitted using eqns (3) and (4) (not shown). The calculated dissociation constants for $I_{act,\infty,rel}$ and s_{rel} are given in Table 1 ($I_{act,\infty}$, s, $K_{D,1}$ and $K_{D,2}$, in 3 mM total Mg, for $hP2X_7$).

N-terminal hexahistidyl tagging and C-terminal truncation diminish receptor activation by the site with low ATP sensitivity

Figure 5*A* and *B* shows typical current traces of the two investigated mutant $hP2X_7$ receptors. Capping the N-terminus with a hexahistidyl sequence reduced the linearly activating and the fast deactivating current components in relation to the exponentially activating and the slowly deactivating current components, respectively (cf. Figs 1*C* and 5*A*). The additional truncation of the last 156 amino acids of the intracellular

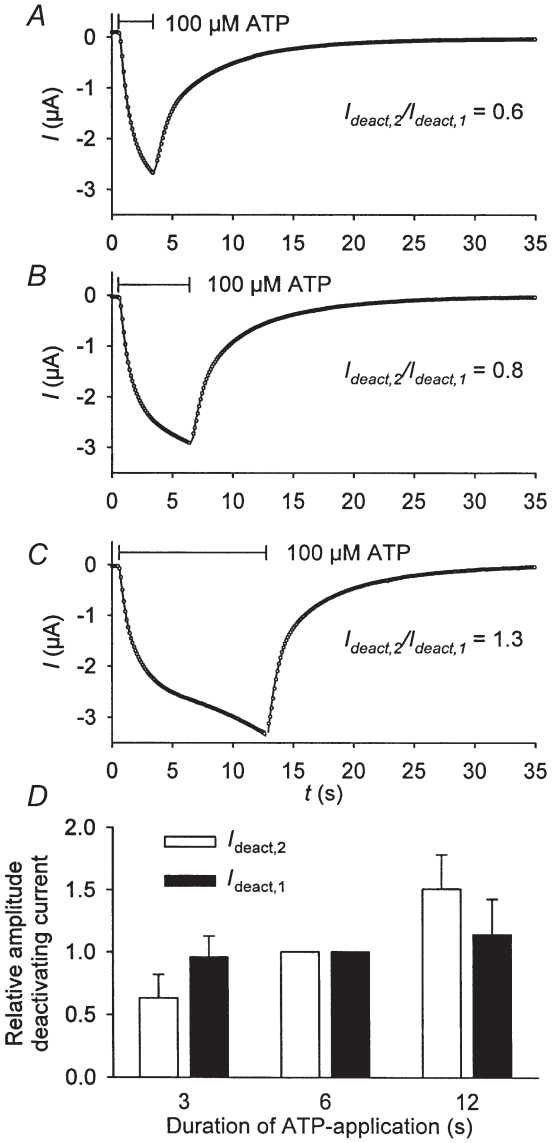

Figure 4. Dependence of the deactivation time course on the duration of agonist application

A–C, examples of $hP2X_7$-dependent currents evoked by increasing duration of ATP application. The relation of the amplitudes of the fast to slow deactivating current, respectively, are given as insets. Divalent cation-free oocyte Ringer solution was used. *D*, statistics of recordings from 8 oocytes performed like those shown in *A–C*, the fast ($I_{deact,2}$, □) and slow ($I_{deact,1}$, ■) deactivating current components, respectively, were normalised to the value measured after application of 0.1 mM ATP for 6 s. Only the means for $I_{deact,2}$ are significantly different.

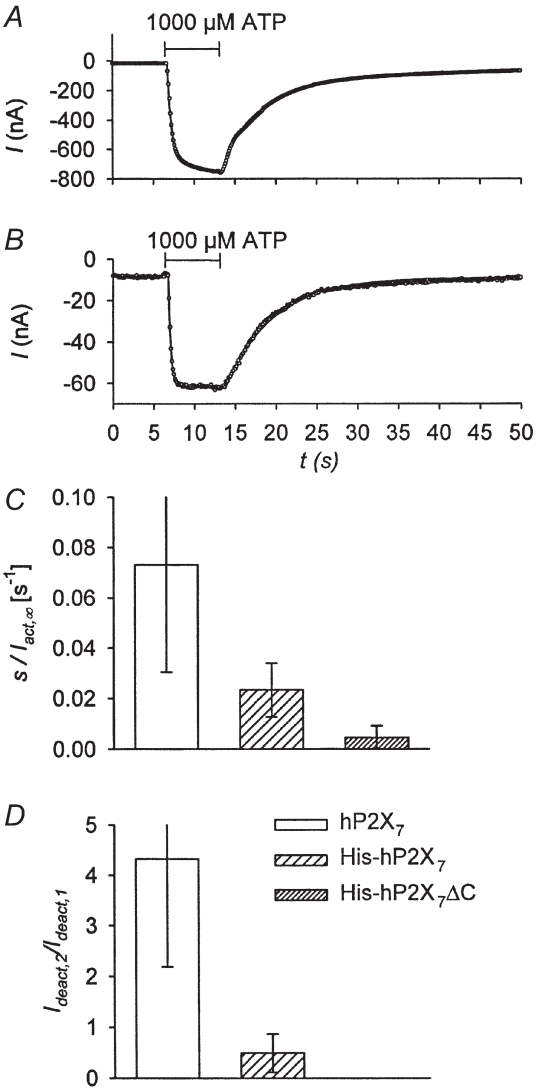

Figure 5. Kinetics of mutated $hP2X_7$ receptors

A and *B*, examples of ATP-activated currents of His-$hP2X_7$ and His-$hP2X_7\Delta C$, respectively. The relation of the slope of the linearly activating current to the steady-state amplitude of the exponentially activating current, $s/I_{act,\infty}$, was calculated as 0.019 and 0.0006 s^{-1} and the relation of the initial amplitudes of the fast and slow deactivating current, $I_{deact,2}/I_{deact,1}$, was determined as 0.4 and 0.0 for *A* and *B*, respectively. For further explanation, see Fig. 1. *C*, relation of the slope of the linearly (s) to the exponentially ($I_{act,\infty}$) activating current approximated according to eqn (1). *D*, relation of the amplitudes of the fast ($I_{deact,2}$) to the slow ($I_{deact,1}$) deactivating current as fitted by eqn (2). Currents were activated by 1 mM ATP in divalent-free oocyte Ringer solution. The means (from 9 to 25 oocytes) are statistically different in *C* and *D*.

C-terminal tail of the $P2X_7$ receptor, which is 239 amino acid residues long, led to a complete disappearance of both the slowly activating and the fast deactivating current components (Fig. 5*B*; for statistical analysis, see Fig. 5*C* and *D*). According to these observations, the low-sensitivity part of the $I_{act,\infty}$–[ATP] relationship is strongly reduced, compared to the high-sensitivity part, for His-$hP2X_7$ (Fig. 6*A*) and is nearly abolished for His-$hP2X_7\Delta C$ (Fig. 6*C*). Nevertheless, the K_D values of both activation sites are not changed (for statistics, see Table 1) Additionally, Mg^{2+} apparently reduces the affinity of the high-sensitivity activation site for total ATP in both mutants (Fig. 6*B* and *C*). Therefore, the binding characteristics of the high-sensitivity activation sites are not obviously altered by the manipulations performed on the N- and C-terminal domains.

The characteristics of the two activation sites at $hP2X_7$ are summarised in Table 1. The mean pK_D for ATP^{4-} at the high-sensitivity site for all three types of $hP2X_7$ receptor is 5.3 ± 0.3 corresponding to 4 μM ATP^{4-}. For the low-sensitivity site, an average pK_D value of 3.7 ± 0.2 corresponding to 220 μM ATP^{4-} was calculated as an average of all determinations.

DISCUSSION

The experimental model

Some limitations of the experimental model used should be considered.

(i) The experiments were generally carried out in divalent cation-free external solutions to attain the high concentrations of ATP^{4-} required to saturate the low-sensitivity site as far as possible. However, control measurements showed that the two distinct ATP^{4-}-dependent activation sites including the described current components could also be found in Ba^{2+}- or Mg^{2+}-containing solutions.

(ii) Some of our kinetic data are influenced to a certain extent by the rate of solution exchange, which is in the range of 1.2 s and 1.8 s (10–90 % exchange times) for the wash-in and wash-out, respectively (Klapperstück *et al.* 2000). This indicates that the speed of solution exchange was rate limiting for the time course of current activation at > 10 μM ATP^{4-} and also for the fast deactivating current component (Fig. 1*D*). Therefore, possible different time courses of the exponentially activating

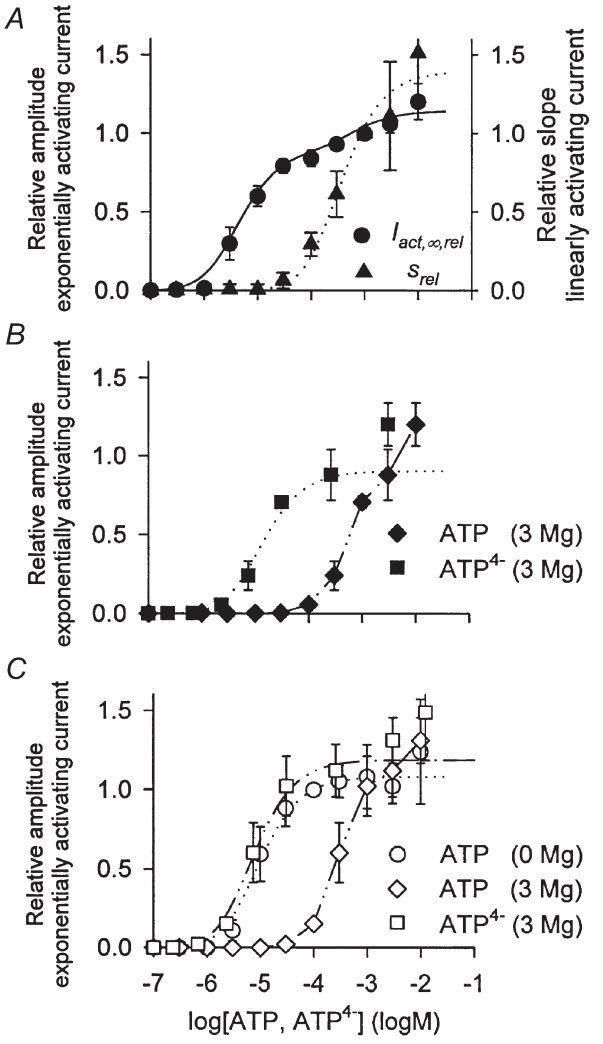

Figure 6. Characterisation of the activation of the modified $hP2X_7$ clones, His-$hP2X_7$ and His-$hP2X_7\Delta C$

A, concentration–response curve for His-$hP2X_7$ of the steady-state activating current ($I_{act,\infty}$, ●) and the slope of the linearly activating current (s, ▲) normalised to the respective component at 1 mM ATP (in divalent-free oocyte Ringer solution). *B*, dependence of $I_{act,\infty,rel}$ of His-$hP2X_7$ on the total ATP concentration in extracellular solution containing 3 mM total Mg (◆) normalised to the values obtained at 1 mM ATP (in divalent cation-free oocyte Ringer solution). This concentration–response curve was recalculated and redrawn using the ATP^{4-} concentration as agonist (■). Data points represent means from between 5 and 25 oocytes. Mean data were approximated by eqn (3) (dotted line) or eqn (4) (continuous line). *C*, characterisation of the activation of His-$hP2X_7\Delta C$. ○, concentration–response curve of the steady-state activating current ($I_{act,\infty}$) normalised to this current at 0.1 mM ATP (divalent cation-free oocyte Ringer solution). ◇, the dependence of $I_{act,\infty}$ on the total ATP concentration in extracellular solution containing 3 mM total Mg normalised to the values obtained at 0.1 mM ATP (in divalent cation-free oocyte Ringer solution). □, this concentration–response curve was recalculated and redrawn using the ATP^{4-} concentration as agonist. Data points represent means from between 5 and 8 oocytes. The calculated dissociation constants are given in Table 1 (see His-$hP2X_7$ and His-$hP2X_7\Delta C$).

current components corresponding to the high- or low-sensitivity sites as well as a possible sigmoidal onset of current activation could not be resolved by our setup. Moreover, we cannot exclude the possibility that the fast deactivating current component has a time constant < 1 s. Despite these restrictions, we believe that our data are not influenced by the speed of solution exchange for the following reasons. Firstly, the steady-state values of the exponentially activating current components and the slope of the linearly activating current component are determined after completion of the solution exchange. Secondly, the time constant of 5 s is slow enough to determine the amplitude of the slowly deactivating current component with reasonable precision, and furthermore allows a sufficiently good distinction between fast and slowly deactivating currents.

(iii) Another matter of concern is that Hill coefficients of 2 were needed to describe the concentration–response curves of the amplitudes of the current components of both activation sites, whereas the kinetic model of activation and deactivation (eqn (1)) corresponds to only one activation site. Therefore, the model of the current kinetics should be considered as a general description of the activation and deactivation time course. Nevertheless, the concentration dependencies of the steady-state values of the activating and the initial values of the deactivating current components are not dependent on the number of activation sites used in the model of current kinetics.

The concentration–response curves could be best described with the highest correlation if Hill coefficients of 2 were used. However, in most cases, models with Hill coefficients of 1 or 3 were not significantly inferior. Therefore, we feel that the number of activation sites cannot be determined reliably by Hill plots alone as shown in this report. Thus, if it is assumed that every subunit of the hP2X$_7$ receptor protein forms one activation site for ATP, our results are not incompatible with the recent finding that three subunits may form complete P2X receptors (Nicke *et al.* 1998).

(iv) High concentrations of ATP induce a very slowly activating current component described as a linearly activating current. As shown previously (Klapperstück *et al.* 2000), this current component does not reach a steady-state value within 2 min of agonist application. We found that even longer applications for up to 5 min did not saturate this component (data not shown). Since prolonged activation of large inward currents often harms oocytes, the slope of the linearly activating current component was used for quantification, although the use of non-steady-state values for analysis by the Hill equation is of questionable value. Thus, the calculated K_D value should be interpreted only as an estimate of the concentration dependence of this slowly activating current component.

The molecular mechanism underlying the linearly activating current component is not clear. Hill plot analysis may be justified if the hP2X$_7$ receptor, once activated by binding ATP to both types of activation site, induces the slow rise of the cation conductance for which the extracellular ATP concentration is not rate limiting. A continuous activation of the low-sensitivity activation sites seems absolutely necessary for the maintenance of this additional conductance, since it is rapidly lost by the removal of ATP. Single channel analysis may be helpful to provide insights into the mechanism of hP2X$_7$ activation at the single molecular level.

Characteristics of the two activation sites

It remains unclear if the induction of the current components which appear at high ATP concentrations needs the occupation of both activation sites or of the low-sensitivity activation sites only. To address this question, the high-sensitivity sites should be blocked by specific antagonists or site directed mutations. But this has not been possible to date because specific antagonists are not available and the structure of the ATP^{4-} activation sites is unknown.

A similar K_D value of about 0.2 mM ATP^{4-} was determined for: (i) the linearly activating current component; (ii) the second exponentially activating current; (iii) the fast deactivating current. The simplest model would assume that these three current components are mediated by occupation of the same low-sensitivity site. This conclusion is supported by the fact that the slope of the linearly activating current and the amplitude of the fast monoexponential decay are strongly correlated with each other. There are at least two possible explanations for the existence of the two different types of ATP^{4-} activation sites. Firstly, the hP2X$_7$ receptor carries an activation site with intrinsically low affinity for ATP^{4-}. Secondly, ATP^{4-} activation sites have initially the same affinity, but the first occupation of an activation site with the negatively charged ATP^{4-} molecules hampers the binding of further ATP^{4-} molecules. That means negative cooperativity would be responsible for the biphasic concentration–response curve.

The rightward shifts of the ATP concentration–response relationship elicited by Ba^{2+} or Mg^{2+} can best be explained by the assumption that both activation sites accept ATP^{4-} only. This conclusion is supported by the fact that ATP activates hP2X$_7$ in the absence of any divalent cations. The dependence on ATP^{4-} is typical of P2Z and P2X$_7$ receptors (Di Virgilio *et al.* 1998).

N- and C-terminal domains play a role in receptor activation

It is interesting that the capping of the N-terminus of the hP2X$_7$ subunit with a hexahistidyl tag greatly reduced the current induced by the activation of the site with low sensitivity to ATP^{4-}. In contrast, currents elicited by the activation of the highly ATP^{4-} sensitive site seem not to be affected. Moreover, the K_D values at the high- and low-sensitivity sites were the same for the wild-type P2X$_7$

receptor and the mutant. This indicates that the ATP^{4-} sensitivity of these mutant $P2X_7$ receptor is not altered, consistent with the exclusive modification at cytosolic domains and the extracellular location of the ATP^{4-} activation site.

The His-tagged mutant with additional truncation of about half of the long C-terminal tail (His-h$P2X_7\Delta C$) shows a kinetic behaviour over the entire ATP^{4-} concentration range, which can be solely attributed to the presence of one single highly ATP^{4-}-sensitive site. Even high ATP^{4-} concentrations are unable to induce the linearly activating current component.

Altogether, this indicates that the effects of ATP^{4-} at the low-sensitivity activation site are mediated, at least in part, by the N- as well as the C-terminal domains. The evaluation of the function of the N-terminus and the C-terminus, however, requires a more detailed analysis at the molecular level.

Physiological relevance of the two types of ATP activation sites

The biphasic characteristics of the concentration–response curve for the $P2X_7$ receptor have not been described before. One reason might be that the current component activated by the highly ATP^{4-}-sensitive site is small in the presence of low concentrations of divalent cations and hence may have remained undetected.

Furthermore, in extracellular solutions containing millimolar concentrations of divalent cations, such as Mg^{2+} and/or Ca^{2+}, the concentration ranges of ATP^{4-} at which the two different types of activation sites are activated are less well separated, that is the ATP concentration–current relation becomes steeper (see Fig. 3*C*). This also hampers the identification of the two different activation sites.

The reported EC_{50} values for concentration–current relationships of the h$P2X_7$ or the human P2Z receptor can be recalculated to K_D values between 45 and 80 μM ATP^{4-} (with $EC_{50} \sim 2.4K_D$ for our model; for calculation of total ATP, see Methods; Bretschneider *et al.* 1995; Markwardt *et al.* 1997; Chessell *et al.* 1998). This means that these values range between the K_D values for the high- and low-sensitivity site calculated in the present work. It is conceivable that Ca^{2+} (which was between 0.3 and 2 mM in the extracellular solution of these reported experiments) may relatively increase the current components of the high-sensitivity activation sites, as Ba^{2+} did in the present experiments (cf. Figs 2*A* and 3*B*). This would result in a shift of the EC_{50} of the whole ATP^{4-} concentration–current curve towards the K_D value of the high-sensitivity site. In divalent cation-free extracellular solutions, the importance of the current components induced by the high-sensitivity site may be small. Therefore, the EC_{50} will be closer to the K_D value of the low-sensitivity activation site. This may explain the higher EC_{50} for ATP^{4-} found in divalent cation-free extracellular solutions (Klapperstück *et al.* 2000).

Studies to investigate the activation and deactivation time course have lacked detailed analysis. They may have been hampered by the fact that most voltage-clamp analyses of $P2X_7$ receptor-dependent currents have been carried out in HEK293 cells, where prolonged or repeated application of agonists can induce large pores in the cell membrane. This leads to a further variable current component which deactivates slowly (Surprenant *et al.* 1996; Rassendren *et al.* 1997; Chessell *et al.* 1998).

In cell culture media (RPMI) containing about 0.5 mM Ca^{2+} and 0.5 mM Mg^{2+}, the dissociation constants determined for ATP^{4-} of about 4 and 220 μM correspond to EC_{50} values for total ATP concentrations of about 120 μM and 3 mM, respectively (see above). It is therefore tempting to speculate that the effects on immune cells of ATP in the low concentration range (see Introduction) are mediated by the high-sensitivity site, whereas the cytolytic effects are only observed after additional occupation of the low-sensitivity ATP activation sites. However, the measurements of rather complex cell reactions to ATP, as mentioned in the Introduction, are not suitable for determining the ATP affinities of the $P2X_7$ receptor. To distinguish between biological effects of the two types of activation sites they should be characterised pharmacologically. Our preliminary results point to different pharmacological profiles. They may be used to distinguish possible different cellular responses which may be ascribed to the occupation of the high-sensitivity only or both ATP^{4-} activation sites. With this in mind, it would be interesting to investigate whether different types of ATP^{4-} activation sites mediate the different effects of low and high concentrations of ATP on the membrane potential, intracellular pH and apoptosis of murine thymocytes (Matko *et al.* 1993; Nagy *et al.* 2000).

Barish, M. E. (1983). A transient calcium-dependent chloride current in the immature *Xenopus* oocyte. *Journal of Physiology* **342**, 309–325.

Bretschneider, F., Klapperstück, M., Löhn, M. & Markwardt, F. (1995). Nonselective cationic currents elicited by extracellular ATP in human B-lymphocytes. *Pflügers Archiv* **429**, 691–698.

Bretschneider, F. & Markwardt, F. (1999). Drug-dependent ion channel gating by application of concentration jumps using U-tube technique. *Methods in Enzymology* **294**, 180–189.

Buell, G., Collo, G. & Rassendren, F. (1996). P2X receptors: an emerging channel family. *European Journal of Neuroscience* **8**, 2221–2228.

Cameron, D. J. (1984). Inhibition of macrophage mediated cytotoxicity by exogenous adenosine 5′-triphosphate. *Journal of Clinical and Laboratory Immunology* **15**, 215–218.

Chessell, I. P., Michel, A. D. & Humphrey, P. P. A. (1998). Effects of antagonists at the human recombinant $P2X_7$ receptor. *British Journal of Pharmacology* **124**, 1314–1320.

Coutinho-Silva, R. & Persechini, P. M. (1997). P2Z purinoceptor-associated pores induced by extracellular ATP in macrophages and J774 cells. *American Journal of Physiology* **273**, C1793–1800.

Di Virgilio, F. (1995). The P2Z purinoceptor: An intriguing role in immunity, inflammation and cell death. *Immunology Today* **16**, 524–528.

Di Virgilio, F., Bronte, V., Collavo, D. & Zanovello, P. (1989). Responses of mouse lymphocytes to extracellular adenosine 5′-triphosphate (ATP). Lymphocytes with cytotoxic activity are resistant to the permeabilizing effects of ATP. *Journal of Immunology* **143**, 1955–1960.

Di Virgilio, F., Chiozzi, P., Falzoni, S., Ferrari, D., Sanz, J. M., Venketaraman, V. & Baricordi, O. R. (1998). Cytolytic P2X purinoceptors. *Cell Death Differentiation* **5**, 191–199.

Dubyak, G. R. & El-Moatassim, C. (1993). Signal transduction via P2-purinergic receptors for extracellular ATP and other nucleotides. *American Journal of Physiology* **265**, C577–606.

El-Moatassim, C., Maurice, T., Mani, J. C. & Dornad, J. (1989). The $[Ca^{2+}]_i$ increase induced in murine thymocytes by extracellular ATP does not involve ATP hydrolysis and is not related to phosphoinositide metabolism. *FEBS Letters* **242**, 391–396.

Ferrari, D., Wesselborg, S., Bauer, M. K. A. & Schulze-Osthoff, K. (1997). Extracellular ATP activates transcription factor NF-kappa B through the P2Z purinoreceptor by selectively targeting NF-κB p65 (Rela). *Journal of Cellular Biology* **139**, 1635–1643.

Filippini, A., Taffs, R. E., Agui, T. & Sitkovsky, M. V. (1990). Ecto-ATPase activity in cytolytic T-lymphocytes. *Journal of Biological Chemistry* **265**, 334–340.

Horn, R. (1987). Statistical methods for model discrimination: Application to gating kinetics and permeation of the acetylcholine receptor channel. *Biophysical Journal* **51**, 255–263.

Jamieson, G. P., Snook, M. B., Thurlow, P. J. & Wiley, J. S. (1996). Extracellular ATP causes loss of l-selectin from human lymphocytes via occupancy of P2Z purinoceptors. *Journal of Cellular Physiology* **166**, 637–642.

Klapperstück, M., Büttner, C., Böhm, T., Schmalzing, G. & Markwardt, F. (2000). Characteristics of P2X$_7$ receptors from human B lymphocytes expressed in *Xenopus* oocytes. *Biochimica et Biophysica Acta* **1467**, 444–456.

Lammas, D. A., Stober, C., Harvey, C. J., Kendrick, N., Panchalingam, S. & Kumararatne, D. S. (1997). ATP-induced killing of mycobacteria by human macrophages is mediated by purinergic P2Z (P2X7) receptors. *Immunity* **7**, 433–444.

MacKenzie, A. B., Surprenant, A. & North, R. A. (1999). Functional and molecular diversity of purinergic ion channel receptors. *Annals of the New York Academy of Sciences* **868**, 716–729.

Markwardt, F., Löhn, M., Böhm, M. & Klapperstück, M. (1997). Purinoceptor-operated cationic channels in human B lymphocytes. *Journal of Physiology* **498**, 143–151.

Matko, J., Nagy, P., Panyl, G., Vereb, G. Jr, Bene, L., Matyus, L. & Damjanovich, S. (1993). Biphasic effect of extracellular ATP on the membrane potential of mouse thymocytes. *Biochemical and Biophysical Research Communications* **191**, 378–384.

Nagy, P. V., Feher, T., Morga, S. & Matko, J. (2000). Apoptosis of murine thymocytes induced by extracellular ATP is dose- and cytosolic pH-dependent. *Immunology Letters* **72**, 23–30.

Nicke, A., Bäumert, H. G., Rettinger, J., Eichele, A., Lambrecht, G., Mutschler, E. & Schmalzing, G. (1998). P2X$_1$ and P2X$_3$ receptors form stable trimers: a novel structural motiv of ligand-gated ion channels. *EMBO Journal* **17**, 3016–3028.

Ralevic, V. & Burnstock, G. (1998). Receptors for purines and pyrimidines. *Pharmacological Reviews* **50**, 413–492.

Rassendren, F., Buell, G. N., Virginio, C., Collo, G., North, R. A. & Surprenant, A. (1997). The permeabilizing ATP receptor, P2X7-cloning and expression of a human cDNA. *Journal of Biological Chemistry* **272**, 5482–5486.

Sanger, F., Nicklen, S. & Coulson, A. R. (1977) DNA sequencing with chain-terminating inhibitors. *Proceedings of the National Academy of Sciences of the USA* **74**, 5463–5467.

Schilling, W. P., Wasylyna, T., Dubyak, G. R., Humphreys, B. D. & Sinkins, W. G. (1999). Maitoxin and P2Z/P2X7 purinergic receptor stimulation activate a common cytolytic pore. *American Journal of Physiology* **277**, C766–776.

Schmidt, A., Ortaldo, J. R. & Herberman, R. B. (1984). Inhibition of human natural killer cell reactivity by exogenous adenosine 5′-triphosphate. *Journal of Immunology* **132**, 146–150.

Schubert, R. (1990). A program for calculating multiple metal-ligand solutions. *Computer Methods and Programs in Biomedicine* **33**, 93–94.

Soto, F., Garcia-Guzman, M. & Stühmer, W. (1997). Cloned ligand-gated channels activated by extracellular ATP (P2X receptors). *Journal of Membrane Biology* **160**, 91–100.

Surprenant, A., Rassendren, F., Kawashima, E., North, R. A. & Buell, G. (1996). The cytolytic P2Z receptor for extracellular ATP identified as a P2X receptor (P2X7). *Science* **272**, 735–738.

Virginio, C., MacKenzie, A., North, R. A. & Surprenant, A. (1999). Kinetics of cell lysis, dye uptake and permeability changes in cells expressing the rat P2X$_7$ receptor. *Journal of Physiology* **519**, 335–346.

Weber, W. M., Liebold, K. M., Reifarth, F. W., Uhr, U. & Clauss, W. (1995). Influence of extracellular Ca^{2+} on endogenous Cl^- channels in *Xenopus* oocytes. *Pflügers Archiv* **429**, 820–824.

Yisraeli, J. K. & Melton, D. A. (1989). Synthesis of long, capped transcripts in vitro by SP6 and T7 RNA polymerases. *Methods in Enzymology* **180**, 42–50.

Zanovello, P., Bronte, V., Rosato, A., Pizzo, P. & Di Virgilio, F. (1990). Responses of mouse lymphocytes to extracellular ATP . II. Extracellular ATP causes cell type-dependent lysis and DNA fragmentation. *Journal of Immunology* **145**, 1545–1550.

Zhang, Y., McBride, D. W. Jr & Hamill, O. P. (1998). The ion selectivity of a membrane conductance inactivated by extracellular calcium in *Xenopus* oocytes. *Journal of Physiology* **508**, 763–776.

Corresponding author

F. Markwardt: Julius-Bernstein-Institut für Physiologie, Martin-Luther-Universität Halle-Wittenberg, Magdeburger Straße 6, D-06097 Halle/Saale, Germany.

Email: fritz.markwardt@medizin.uni-halle.de